EXTRACTION OF MAN-MADE FEATURES BY 3-D ACTIVE CONTOUR MODELS

John C. Trinder
School of Geomatic Engineering
The University of New South Wales
Sydney NSW 2052, Australia

Haihong Li
Institute of Geodesy & Photogrammetry
Swiss Federal Institute of Technology
ETH - Hoenggerberg, CH-8093, Zurich, Switzerland

ISPRS Commission III, Working Group 2

KEY WORDS: Feature, Extraction, Remote_Sensing, Vision, Software, Digital.

ABSTRACT

This paper describes the principles and procedures for the implementation of a semi-automatic method for the extraction of linear features on remotely sensed satellite and aerial images in 2D and 3D, based on active contour models or 'snakes'. Snakes are a method of interpolation by regular curves to represent linear features on images. The procedure requires the initial extraction of the locations of elements of linear features in a remotely sensed image by appropriate image processing methods. The assistance of an operator is required to locate points along and near the feature. The iterative computation then locates the feature as closely as the details in the image will allow. For aerial photography, the procedure extracts both sides of the roads. Results of tests of the extraction of linear features on SPOT satellite images and aerial photography are described in terms of the relative accuracy of the extracted features, for a range of features, for both 2 dimensional and 3 dimensional geometry, and the absolute accuracy in 3D of the extracted features.

1. INTRODUCTION

Linear feature extraction has been carried out on remotely sensed digital images for many years with varying degrees of success. The extraction of features from digital remotely sensed data must be based on the determination of sufficient attributes in the image to ensure their correct location. Typical attributes include tone, size, texture, shadow and characteristics of the site in which the feature occurs, ie context. Most attempts to extract features have commenced using 'low level' processes based on radiometric characteristics of the images, such as edge detector algorithms, because the features are revealed by their contrast with respect to their background. This is followed by additional processes to link or track the feature components in the image.

Low level image processing, using primarily the gradients of edges derived in small windows in the image, is effectively one dimensional, and does not take into account the structure or shape of the feature, nor does it consider the essential attributes, of other aspects of geometry, or the context, global and local, within which the feature occurs. Viewers of remotely sensed data are aware of the superiority of experienced human observers over most currently available methods of feature extraction based on low level image processing, and this is clearly because these techniques are crude methods of feature extraction. However, while low level methods do not result in a successful feature extraction scheme, they may be used as an initial step in a successful regime for feature extraction. Recent approaches to feature extraction on remotely sensed images have taken a more comprehensive approach, using image understanding modules based on AI methods, such as expert systems, for object identification and scene description, as has been adopted by a number of researchers in the computer science field eg McKeown et al (1985) and Strat et al (1991). The description of these characteristics on remotely sensed images requires an understanding of the structure of the features themselves as well as their relationships on the ground. Research in this field is still in its early stages.

An interim step in the process of developing fully automatic procedures of feature extraction, is to use a semi-automatic approach in which the approximate location of the feature is determined by the operator, and the algorithm then accurately locates the feature. In this case, the operator is responsible for assessing the context of the image, while the algorithm locates the feature based on the radiometric values as well as its structure. This paper describes the principles and procedures for the implementation of a semi-automatic method for the extraction of linear features on remotely sensed images in 2D and 3D, based on active contour models or 'snakes'. It will include: an explanation of the theory of snakes; the method of implementation of the snakes by B-splines in 2 dimensions (2D) and 3 dimensions (3D) on satellite and aerial images; and tests of these procedures and conclusions.

2. CURVE FITTING ALGORITHM BY SNAKES

2.1 Principles of Snakes

The implementation of feature delineation by snakes from satellite and aerial images, using interactive methods to determine approximate locations, is based on a framework of energy minimisation (Kass et al 1988). Fua and Leclerc (1990) have stated that the snakes method has two advantages: geometric constraints are directly used to guide the search for

the edge; and the edge information is integrated along the whole length of the curve. That is, the method determines the structure of the feature. Fua and Leclerc have developed variations to the method of Kass et al (1988).

Snakes derive their name from the fact that they are splines reacting with an image, which 'slither' around in position during the iterations to determine the feature. The curves used to model linear features in this paper are B-splines. The advantages of the splines are that they are smooth piecewise polynomials which maintain continuity between neighbouring sections or domains. In addition, they have the characteristic that they limit the influence of errors in the points used to locate the curve of order 'n', to 'n+1' domains of the curve. The definition of the B-splines is based on the knowledge of both a set of polynomial functions, which define the shape of the function, and a given set of control points or a control polygon, defined by a number of fixed locations along the curve. The B-spline function adopted is a 3rd order function, while the control polygon is determined from the image details representing the feature. The spline is subject to internal forces, referred to as internal energy, brought about by the inherent piecewise smoothness of the B-spline, while the external forces which relate to the image information, force the snake towards the feature.

The key concept of the algorithm is the minimisation of the total energy which relates to the snake's position. Total energy, the sum of the two kinds of energies : internal and external; is expressed by a parametric representation, $v(s) = (x(s), y(s))$, as

$$\begin{aligned} E &= \int_{s_0}^{s_1} E(v(s))ds \\ &= \int_{s_0}^{s_1} [E_g(v(s)) + E_p(v(s)) + E_c(v(s), v_0(s))]ds \end{aligned} \quad (1)$$

where the internal or geometric energy *Eg* is derived from the geometric constraints of the object model. The photometric or external energy *Ep* represents the forces derived from the image which constrain the snake to the feature of interest. The control energy *Ec* defines the boundary conditions, which constrain the difference between the contour *v(s)* and the initial curve $v_0(s)$.

Normally, **the geometric energy, *Eg*,** is based on the first derivative (v_s) and second derivative (v_{ss}) of the function, which constrain the snake to be a smooth curve, defined by

$$E_g = \alpha |v_s(s)|^2 + \beta |v_{ss}(s)|^2 \quad (2)$$

where α and β are constants which control the influence of the geometric energy against the photometric energy.

The photometric energy *Ep* , derived from the image, depends on the type of features to be extracted. For a narrow linear feature, it can simply be the square of intensity values of the image, multiplied with a positive or negative constant for lighter or darker features respectively. ie,

$$E_{pl} = w|I(x,y)|^2 \quad (3)$$

For a step edge, it can be calculated as,

$$E_{pe} = -|\nabla I(x,y)|^2 \quad (4)$$

thus attracting the snake to image points with high gradient values. In this implementation, the features in the image are defined by morphological tools for narrow features and the Canny operator (Canny 1986) for step functions. The 'energy image' is defined by a Chamfer image, derived from the feature image (see Section 4), in which the pixel values relate to their closeness to any surrounding edge. Letting,

$$E_{ext} = E_p + E_c \quad (5)$$

(1) becomes,

$$\begin{aligned} E &= \int_{s_0}^{s_1} [\alpha |v_s(s)|^2 + \beta |v_{ss}(s)|^2 + E_{ext}(v(s))]ds \\ &= \int_{s_0}^{s_1} F(s, v, v_s, v_{ss})ds \end{aligned} \quad (6)$$

The computation requires the minimisation of this energy.

However, for the solution of this algorithm, there is a need to determine estimates of high order derivatives, which is a typical ill-posed problem and may cause instabilities. Instead, the snake can be embedded in a viscous medium and the equations of dynamics solved (Fua et al. 1990),

$$\frac{\partial}{\partial X} E + \lambda \frac{d}{dt} X = 0 \quad (7a)$$

$$\frac{\partial}{\partial Y} E + \lambda \frac{d}{dt} Y = 0 \quad (7b)$$

2.2 Approximation by a Cubic Spline

Suppose a snake can be approximated by a cubic spline. That is,

$$x(s) = \sum_{i=1}^{n} N_i(s) X_i \quad (8a)$$

$$y(s) = \sum_{i=1}^{n} N_i(s) Y_i \quad (8b)$$

where X_i and Y_i are the parameters of the cubic spline in x and y directions in the image respectively, and $N_i(s)$ is the normalised cubic B-spline between knots s_i and s_{i+4}. For equally spaced simple knots, with a spacing h,

$$N_i(s) = \begin{cases} s^3/6h^3 & 0 \le s - s_i \le h \\ (1 + 3s + 3s^2 - 3s^3)/6h^3 & h \le s - s_i \le 2h \\ (4 - 6s^2 + 3s^3)/6h^3 & 2h \le s - s_i \le 3h \\ (1 - 3s + 3s^2 - s^3)/6h^3 & 3h \le s - s_i \le 4h \end{cases} \quad (9)$$

In the actual implementation, the snake is located at discrete values so that the integration of the B-spline in (1) will be replaced with a summation. Letting,

$$N = [N_1(s)\ N_2(s)\ \ldots\ N_n(s)] \quad (10a)$$

$$N_s = [N_1'(s)\ N_2'(s)\ \ldots\ N_n'(s)] \quad (10b)$$

$$N_{ss} = [N_1''(s)\ N_2''(s)\ \ldots\ N_n''(s)] \quad (10c)$$

$$X = [X_1\ X_2\ \ldots\ X_n]^T \quad (11a)$$

$$Y = [Y_1\ Y_2\ \ldots\ Y_n]^T \quad (11b)$$

$$E_p = [f(x,y)]^T [f(x,y)] \quad (11c)$$

the total energy can be written in matrix form as,

$$E = \alpha Y^T N_s^T N_s X + \beta X^T N_{ss}^T N_{ss} X + \alpha Y^T N_s^T N_s Y + \beta Y^T N_{ss}^T N_{ss} Y + [f(x,y)]^T [f(x,y)] + E_c \quad (12)$$

To minimise this energy in (12), the conditions are:

$$\frac{\partial}{\partial X} E = \frac{\partial}{\partial Y} E = 0 \quad (13)$$

Hence

$$(\alpha N_s^T N_s + \beta N_{ss}^T N_{ss}) X + N^T [f_x(x,y)]^T [f(x,y)] + \frac{\partial}{\partial X} E_c = 0 \quad (14a)$$

$$(\alpha N_s^T N_s + \beta N_{ss}^T N_{ss}) Y + N^T [f_y(x,y)]^T [f(x,y)] + \frac{\partial}{\partial Y} E_c = 0 \quad (14b)$$

In a semi-automatic feature extraction scheme, the operator initially places a curve near the image structure of interest. By this initial curve, the approximations X_0 and Y_0 of X and Y can be calculated. The goal is therefore to find the corrections ΔX and ΔY such that,

$$X = X_0 + \Delta X \quad (15a)$$

$$Y = Y_0 + \Delta Y \quad (15b)$$

Letting $B = \alpha N_s^T N_s + \beta N_{ss}^T N_{ss}$ (16)

and following appropriate substitutions, based on the assumption that the initial curve is located on the feature, the final set of equations become

$$(B + N^T [f_x(x_0,y_0)]^T [f_x(x_0,y_0)] N + \lambda I) \Delta X + N^T [f_x(x_0,y_0)]^T [f(x_0,y_0)] = 0 \quad (17a)$$

$$(B + N^T [f_y(x_0,y_0)]^T [f_y(x_0,y_0)] N + \lambda I) \Delta Y + N^T [f_y(x_0,y_0)]^T [f(x_0,y_0)] = 0 \quad (17b)$$

3. 3-D FEATURE EXTRACTION BY SNAKES

If a feature is extracted from more than one image, its coordinates in 3-D space can be computed. Suppose a snake in 3-D space, in the coordinates defined by the ground system, can be approximated by a cubic B-spline. That is,

$$X(s) = \sum_{i=1}^{n} N_i(s) X_i$$
$$Y(s) = \sum_{i=1}^{n} N_i(s) Y_i \quad (18)$$
$$Z(s) = \sum_{i=1}^{n} N_i(s) Z_i$$

From the camera models for each image, derived for the particular acquisition system being used, either satellite sensor or aerial camera, projection equations which describe the relationships between the image and ground coordinate systems can be written as,

$$x_i(s) = P_{xi}(X(s), Y(s), Z(s))$$
$$y_i(s) = P_{yi}(X(s), Y(s), Z(s)) \quad (19)$$

where $x_i(s)$ and $y_i(s)$ are the coordinates of the snake on the *ith* image.

The external energy of the snake can now be defined as a sum of energies on each image,

$$E_{ext} = E_{ext}(x_1(s), y_1(s)) + \ldots + E_{ext}(x_m(s), y_m(s)) = [F_1 \; F_2 \; \ldots \; F_m][F_1 \; F_2 \; \ldots \; F_m]^T = F^T F \quad (20)$$

where F is an expression for energy for 3D images.

In a similar manner to the derivation in Section 2, the formula for 3-D snakes is, (cf. equations 17a, 17b)

$$(B + N^T F_X^T F_X N + \lambda I) \Delta X + N^T F_X^T F = 0 \quad (21a)$$

$$(B + N^T F_Y^T F_Y N + \lambda I) \Delta Y + N^T F_Y^T F = 0 \quad (21b)$$

$$(B + N^T F_Z^T F_Z N + \lambda I) \Delta Z + N^T F_Z^T F = 0 \quad (21c)$$

where F_X, F_Y *and* F_Z are partial derivatives and can be derived from the equations 19 and 20,

$$F_X = \left[\frac{\partial F_1}{\partial x_1}\frac{\partial P_{x1}}{\partial X} + \frac{\partial F_1}{\partial y_1}\frac{\partial P_{y1}}{\partial X} \quad \ldots \quad \frac{\partial F_m}{\partial x_m}\frac{\partial P_{xm}}{\partial X} + \frac{\partial Fm}{\partial ym}\frac{\partial Pym}{\partial X} \right]^T \quad (22a)$$

$$F_Y = \left[\frac{\partial F_1}{\partial x_1}\frac{\partial P_{x1}}{\partial Y} + \frac{\partial F_1}{\partial y_1}\frac{\partial P_{y1}}{\partial Y} \quad \ldots \quad \frac{\partial F_m}{\partial x_m}\frac{\partial P_{xm}}{\partial Y} + \frac{\partial Fm}{\partial ym}\frac{\partial Pym}{\partial Y} \right]^T \quad (22b)$$

$$F_Z = \left[\frac{\partial F_1}{\partial x_1}\frac{\partial P_{x1}}{\partial Z} + \frac{\partial F_1}{\partial y_1}\frac{\partial P_{y1}}{\partial Z} \quad \ldots \quad \frac{\partial F_m}{\partial x_m}\frac{\partial P_{xm}}{\partial Z} + \frac{\partial Fm}{\partial ym}\frac{\partial Pym}{\partial Z} \right]^T \quad (22c)$$

With appropriate approximations, the above system can be efficiently in a similar manner to the 2-D snakes.

Seed points of the feature to be extracted should be given by an operator on one of the images, say *ith* image and then the approximation location of the snake in 3-D space can be computed from known relationships between the overlapping images, using the cameras models and a known DEM of the region.

4. IMPLEMENTATION

The processing chain to derive the energy image from the original image is as follows :

- Preprocessing by image stretching
- Edge detection by:
  - Canny operator for single edges, such as dividing lines between features or edges of roads on aerial photography.
  - Morphological tools for narrow features, such as roads on satellite images. To detect bright small elements, erosion followed by a dilation is applied; then the original image is subtracted from this result. For dark small elements, dilation is applied first, then erosion.

- Derivation of a chamfer image in which the pixel values relate to their closeness to any surrounding edge. For example, if an edge pixel has the grey value strength P_e, then for a non-edge pixel located x pixels away from it, its grey value $P_{non\text{-}edge}$ (in the chamfer image) should become P_e minus x. Since there are many edge pixels in an image, the recorded value $P_{non\text{-}edge}$ is the maximum value derived from all edge pixels.

- Compute the snake by equations 17 or 21.

- For features, such as roads with significant width and parallel sides occurring on larger scale aerial photography, both sides of the road need to be detected. The design of the extraction process for roads is based on the extraction of one side of the road, and the automatic determination of the approximate location of the other side of the road from the edge information extracted by the Canny operator. These positions are then used as starting positions of the road edge for the computation of its position by the snake. Iteration of the computations from one side of the road to the other improves the computed final location of both edges of the feature.

5. TESTS ON THE APPLICATION OF SNAKES

Visual tests of the 2D feature extraction process, for a single image, revealed that considerable success was achieved with the procedure, as shown in Figures 1, 2, 3 and 4. While the quality of the extracted features should be dependent on the initial feature extraction procedure, the snake interpolation generally works well when there are no other features close to the feature being extracted, as shown in Figure 1. If there are other nearby features in the image data, the snake may become distorted. This can be partially overcome by the operator locating the feature being extracted as accurately as possible in the region of the other features. If wide features such as roads are located by a single snake, it may jump from one side of the road to the other. In this case, the tool for the parallel features needs to be used, as shown in Figure 3. Tests on the 3D extraction of features, based on two overlapping images, revealed similar results to 2D extraction, with the additional advantage that the 3D coordinates in the ground coordinate system were also determined. Visual comparisons have also been carried out between the method of snakes, and the method of feature extraction based on dynamic programming (Gruen and Li 1994), revealing similar results.

5.1 Tests on Satellite Images

In order to obtain estimates of the quality of the feature extraction on satellite images, a number of tests were carried out on overlapping SPOT images over the Sydney region. The first pair of images, with a B/H of 1.0, was recorded on SPOT1 in 1986. They suffer from poor dynamic range and a considerable level of noise. The second set, with a B/H of 0.6, was recorded 5 months apart in 1994 from SPOT2. One of the images has high dynamic range, while the other suffers from poor dynamic range because of a considerable level of cloud cover. Small regions of cloud also appear on this image. Orthophoto maps in the region with a scale of 1:4,000 and 1m and 2m contours, were used as ground truth information for the 3D extraction. Accuracies of planimetric positions and elevations are of the order of 2m or better on the orthophotos.

The following tests were undertaken.

(i) A study has been made of the effect of the magnitude of the error in the initial position of the feature defined by the operator, on the accuracy of the computed position of the feature (Trinder and Li 1995). This is defined as the 'pull-in range' of the computation. For this test the position of a feature was initially defined manually on the screen as accurately as possible, and the snake computed. The manual location and snake computation were compared, to check the quality of the extraction. This location was then considered as the 'reference' position for that feature for the purposes of tests of the 'pull-in' range. These tests revealed that features derived interactively by an operator within approximately 5 pixels of their correct positions, will generally be located by the snake computation with a relative accuracy of better than 0.5 pixel, or 5 metres on the ground for SPOT images. If the error in the location of the feature is larger than 7 pixels, the relative accuracy of the feature location will deteriorate to greater than 1 pixel. The relative accuracy for 3D extraction was 1 pixel when the input position of the feature was of the order of 5 pixels from its correct position. One of the advantages of using the overlapping images is that it usually overcomes the problems of missing data in one or both images, due to small obstructions, as shown in Figure 3, but its success depends on the extent of the obstruction, and the quality of the edge information.

(ii) Trinder and Li (1995) demonstrated that, as shown in the first 2 lines of Table 1, the absolute accuracy of the 3D feature extraction method, obtained by comparing the E, N and H coordinates of the 3D snake with the map coordinates of the same feature is of the order of 3 m in E and N coordinates and 6m for elevations for the SPOT2 pair of images with a B/H of 0.6, on the flat terrain in the sections of the image tested.

Table 1
Absolute accuracy in metres of extracted 3D features

Image	Coord	No of linear features	No. of points	Absolute Accuracy
SPOT	E and N	12	120	0.3 pixel 3m
SPOT	H	9 (N-S only)	90	6m
photo 1:16,000	E and N	3	40-85	1 pixel, 0.4m
photo 1:16,000	H	3	40-85	0.5m
photo 1:8,000	E and N	3	25-35	0.8 pixel, 0.16m
photo 1:8,000	H	3	25-35	0.2m
photo 1:8,000	E and N	1	30-35	1.8 pixel 0.35m
photo 1:8,000	H	1	30-35	0.52m

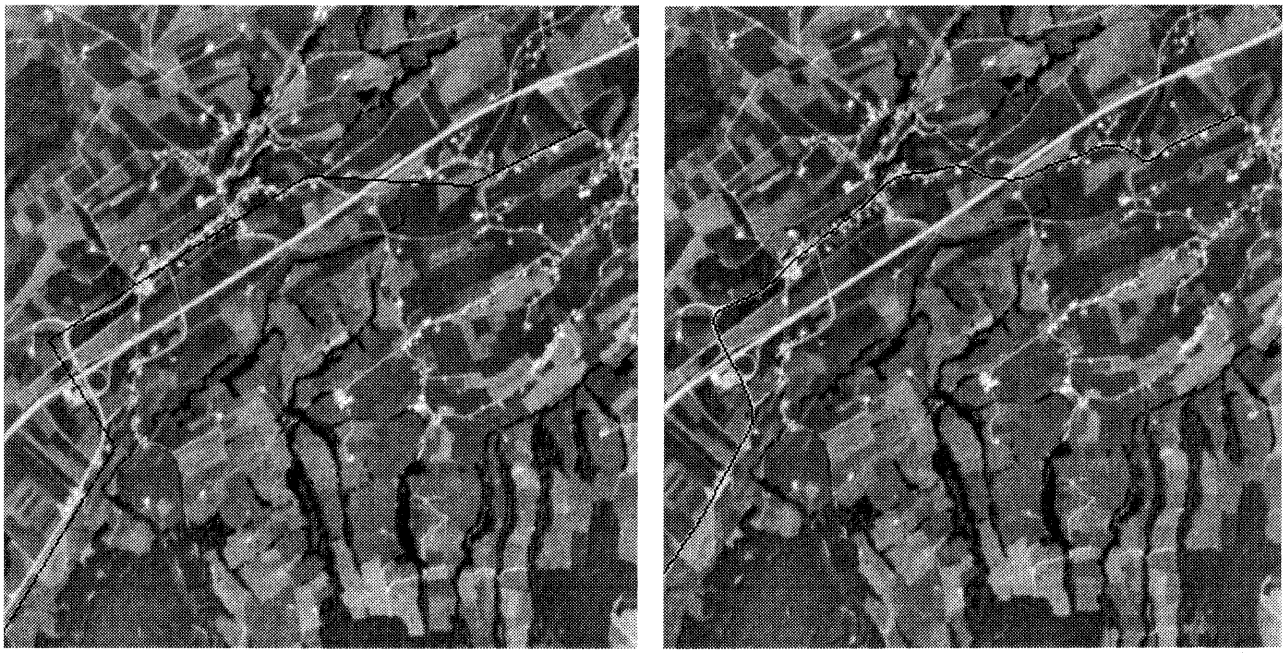

Figure 1. The left image shows the approximate location of the feature by the operator, while the right image shows the location derived by the snakes

5.2 Tests on Aerial Photography

Tests on the extraction of features on overlapping aerial photographs have investigated the absolute accuracy of the features. In this case, the location of the extracted feature has been compared with positions derived from the analogue images observed in an analytical stereoplotter. Three sets of, aerial images were observed at scales of 1:8,000 and 1:16,000 digitised with a pixel size of 25 μm, equivalent to 0.2m and 0.4m on the ground respectively. The accuracy of plotting of features in the Wild BC2 analytical stereoplotter was estimated to be of the order of 10 to 20 μm in the image, between 0.1 to 0.3 m on the object in these cases. Results of these tests are shown in Table 1.

The results of the tests reveal that the accuracy of the extraction of man-made linear features, including single boundaries, both sides of roads and buildings is of the order of 1 pixel, for aerial photography digitised wish a pixel size of 25μm. Elevations of the features are of a similar accuracy to the planimetry. These accuracies are consistent with those obtained by a human observer on analogue images on a stereoplotter.

6. CONCLUSIONS.

(i) The tests revealed that considerable success has been achieved with the method of feature extraction using snakes, particularly for single features which are separated from other features in the image. It combines the skills of the operator and the power of the computer for efficient and accurate extraction of features. However, the method is dependent on the initial feature extraction procedure. As well, if there are other features in the image data nearby, the snake may become distorted.

(ii) The pull-in range of the method can be in excess of 10 pixels for well defined features, but this range should normally be considered as approximately 5 pixels. Under these circumstances, the relative accuracy of the extracted features is of the order of 0.5 pixel for 2D data, and 1 pixel for 3D data. 3D feature extraction is less efficient than 2D extraction, in terms of pull-in range.

(iii) The 3D extraction enables the determination of 3D coordinates of the features and overcome small obstructions on one or both images. The absolute accuracies of this process have been found to be of the order of 3m in E and N and 6m in H on SPOT 10m resolution data. On aerial photography digitised with a pixel size of 25μm, linear features have been extracted with an accuracy of the order of 1 pixel in planimetry and height. Such accuracies are consistent with those obtained by human observers on analogue images.

7. ACKNOWLEDGMENTS

A number of people in addition to the authors of the paper have contributed to this research. Mr Alexis Vuillemin initially developed the procedures for the implementation of the snakes, which were subsequently further developed by Mr Haihong Li. Further code was developed by postgraduate students at UNSW. Mr Yongru Huang developed the software for the 3D snakes, while Mr Yandong Wang applied the snakes to aerial photography. Mr Brian Donnelly provided significant assistance in the provision of the orientations of the images and DEMs. It is acknowledged that the initial investigations of this research were funded by the Electronics Research Laboratory Defence Science and Technology Organisation (DSTO) in Salisbury, South Australia under the direction of Dr Vittala K. Shettigara, while the latter part of the research was supported by a grant from the Australian Research Council in Canberra. Finally acknowledgments are given to the Australian Centre for

Remote Sensing which provided the stereo SPOT images used for some of the tests.

8. REFERENCES

Canny J. (1986) 'A Computational Approach to Edge Detection', IEEE Trans Pattern Analysis and Machine Intelligence PAMI-8 pp 679-698.

Fua P., and Leclerc Y. G. (1990) 'Model Driven Edge Detection', Machine Vision Applications (1990) 3:45-56

Fua P. and Hanson A.J.(1991) 'An Optimization Framework for Feature Extraction', Machine Vision Applications (1991) 4:59-87.

Gruen A. and Li H. (1994) 'Semi-Automatic Road Extraction by Dynamic Programming', International Archives of Photogrammetry and Remote Sensing, Vol. 30-3 pp 324-332.

Huang Y. and Trinder J. (1994) 'A Feature-Based Approach To Reconstruction Of 3-D Objects From Digital Images", International Archives of Photogrammetry and Remote Sensing, Vol. 30-3 pp 391-398.

Kass M., Witkin A., and Terzopoulos D., (1988) 'Snakes: Active Contour Models', Int. Journ. of Computer Vision, Vol 1, pp 321-331.

McKeown, D M, Harvey, W A and McDermott, J (1985) Rule-Based Interpretation of Aerial Imagery, *IEEE Transactions on Pattern Analysis and Machine Perception*, Vol. 7, No.5, pp. 570 - 585.

Rougon N. (1991) 'Kinetics of Interface Evolution with Applications to Active Contour Models', SPIE Vol. 1610 Curve and Surfaces in Computer Vision and Graphics II.

Rougon N. and Prêteux (1991) 'Deformable markers: mathematical morphology for Active Contour Models', SPIE's 1991 International Symposium on Optical Applied Science and Engineering Image. Algebra and Morphological Image Processing II, San Diego, California, Vol. 1568, pp 78-89.

Sperling G. (1970) 'Binocular Vision: A Physical and Neural Theory' Am J. Psychology, Vol 83 pp 461-534.

Strat T. M. and Fischler M.A. (1991) 'Context-Based Vision: Recognizing Objects Using Information from Both 2-D and 3-D Imagery', *IEEE Trans PAMI-13*, pp 1050 - 1065.

Trinder J. C. and Li H. (1995) 'Semi-Automatic Feature Extraction by Snakes' in Automatic Extraction of Man-Made Objects from Aerial and Space Images, A. Gruen, O. Kuebler, P. Agouris (eds), Birkhäuser, Basel 1995.

Williams D.J. and Mubarak Shah (1992), 'A Fast Algorithm for Active Contours and Curvature Estimation', Image Understanding, Vol. 55, No. 1, January, pp 14-26.

Figure 2. Extracted boundary feature on aerial photography

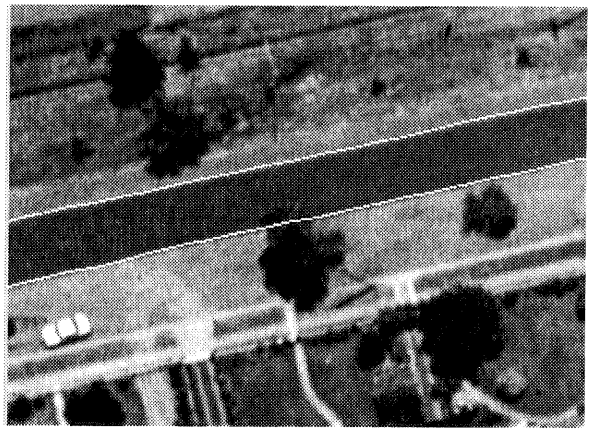

Figure 3. Extracted road boundaries on aerial photography

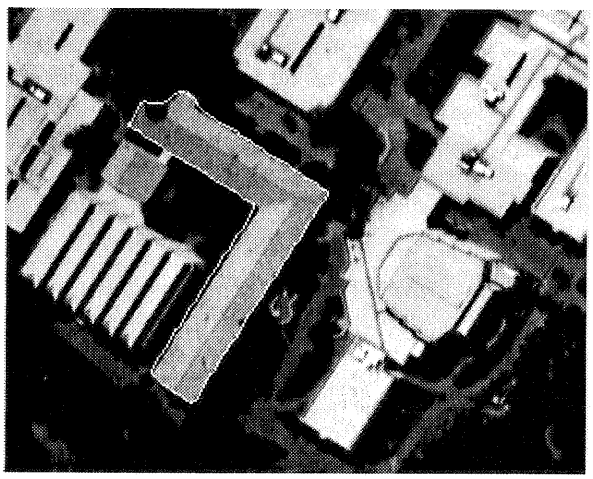

Figure 4. Extracted building on aerial photography